A biomechanical model of index finger dynamics

N. Brook*, J. Mizrahi†, M. Shoham* and J. Dayan*

*Faculty of Mechanical Engineering, Technion – Israel Institute of Technology, Haifa 32000, Israel; †Department of Biomedical Engineering, Technion – Israel Institute of Technology, Haifa 32000, Israel.

Received August 1993, accepted October 1993

ABSTRACT

A dynamic model of the biomechanics of the index finger for flexion-extension and abduction-adduction motion is introduced. The model takes into account all the tendons in the finger and relates to their varying moment arms during motion. A new set of moment arm coefficients and elongation equations is derived based on experimental measurements of previous studies. Constraint equations using variable coefficients are introduced and an optimization approach used to obtain the tendon forces required for any given motion and external force. The model and optimization approach are tested with data from a rapid pinch experiment as well as a hypothetical disc rotation. Good correlation is obtained with respect to electromyographic data in the literature.

Keywords: Finger, hand, biomechanical model, dynamics

Med. Eng. Phys., 1995, Vol. **17**, 54–63, January

NOMENCLATURE

b^m	first order coefficient of excursion model for tendon m.
b_a^m	first order coefficient of excursion model for tendon m during adduction.
d^m	distance from the straight part of tendon m to the long axis of the bone.
DIP	distal interphalangeal joint.
E_m	excursion of tendon m.
E_D	tendon excursion given in data.
EC	extensor digitorum communis.
EI	extensor indicis.
EMG	electromyography.
ES	extensor slip.
F_m	vector of tendon forces.
FDP	flexor digitorum profundus.
FDS	flexor digitorum superficialis.
h^m	second order coefficient of excursion model for tendon m.
h_a^m	second order coefficient of excursion model for tendon m during adduction.
J_c	cost function.
K	elasticity of ligaments in extensor mechanism.
LE	long extensor.
LU	lumbrical.
M_D	average moment arm, given in data.
MP	metacarpophalangeal joint.
n	number of degrees of freedom.
PCSA	physical cross sectional area.
PIP	proximal interphalangeal joint.
r^m	radius of trochlea at crossing of tendon m.
RB	radial band.
RI	radial interosseous.
TE	terminal extensor.
u	number of unknowns.
UB	ulnar band.
UI	ulnar interosseous.
W	matrix of moment arms.
y^m	distance from the straight part of tendon m to the joint axis, measured along the axis of the bone.
α^m	fraction of force of m transmitted to the lateral bands.
β^m	geometric constant relating excursion of m to that of TE.
γ	angle of palm with respect to vertical plane.
δ	joint rotation angle.
ϵ^m	relative motion between m and ES.
θ	adduction angle.
τ	vector of joint moments.
ϕ_i	flexion angle of joint i.
χ	cosine term for tendon angle of convergence.

Correspondence and reprint requests to: J. Mizrahi, Dept of Biomedical Engineering, Technion IIT, Haifa 32000, Israel.

1350-4533/95/01054-10

INTRODUCTION

Models of the human hand are of great importance, in the biomedical, medical ergonomic and robotic fields. These models are constructed to predict the muscle and tendon forces used while grasping, to explore important considerations in reconstructive surgery and to predict grip and manipulation postures. Hand functions can be divided into those where the hand immobilizes an object and those where an object is manipulated in the hand. Both static and dynamic analyses of forces in the hand are, therefore, of importance.

The kinematic skeleton of the human finger, can be mathematically approximated as ideal revolute joints connected by rigid links. The two interphalangeal joints proximal (PIP) and distal (DIP), are described as hinge joints capable of only flexion and extension. The metacarpophalangeal joint (MP) is a saddle joint capable of both flexion – extension and abduction – adduction motions (see *Figure 1*).

Every finger in the hand is controlled by no less than six muscles, nine maximum in the fifth and seven in the index finger. The major extrinsic flexors and extensors are joined by intrinsics of the hand to create a highly complex anatomical structure. The major complexity is in the extensor mechanism responsible for interphalangeal coordination (*Figure 2*).

The strength of the finger is dependent upon the anatomical structure and the maximum effort of each individual muscle involved. Chao *et al.*[1] used a three dimensional model to analyze the forces at all three finger joints during tip lateral and ulnar pinch and during grasp. Tendon positions were found using bi-planar radiography on cadaver fingers. Six equilibrium equations were obtained from each joint yielding a total of 18 equations for the index finger. A total of 24 unknown variables was considered, thus making the problem statically indeterminate with 6 degrees of redundancy. Four additional constraint equations, based on the anatomical structure of the musculotendinous mechanism, were incorporated, as well as six inequality constraints specifying the upper limits of muscle strength based on physiological cross-sectional area (PCSA). The statically indeterminate problem was solved using the permutation/combination principle. Systematically combining the redundant variables and solving for the remaining ones, resulted in 126 possible solutions. These were reduced in number by discarding those with compressive tendon forces, tensile joint forces, excess joint forces or excessive extensor forces. The final results were the average of the remaining possible solutions. For an external force of magnitude P, joint reaction forces of $5.6P$, $6P$ and $8.8P$ were reported for the DIP, PIP and MP joints of the index finger, respectively.

Chao and An[2], suggested using both permutation/combination and the linear programming techniques. Several objective functions were suggested. It was further shown that the pinch strength depends on the direction of the applied force as well as the joint orientation.

Berme *et al.*[3], studied index finger MP joint forces during pinching and tap turning activities, using a 3-dimensional model. The flexor apparatus was simplified to a single notional 'flexor tendon'. Six female cadaver specimens were dissected, marked and photographed from various angles, to locate the major force carrying elements, with the MP at four different angles of

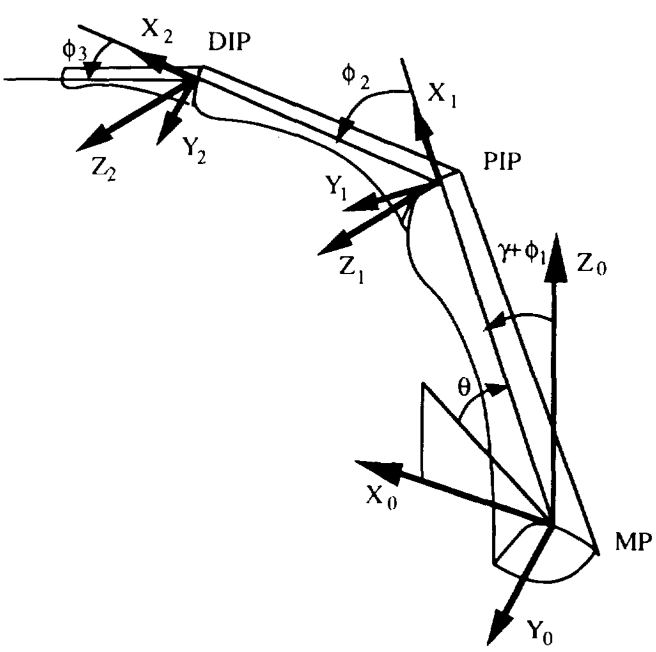

Figure 1 Schematic representation of index finger

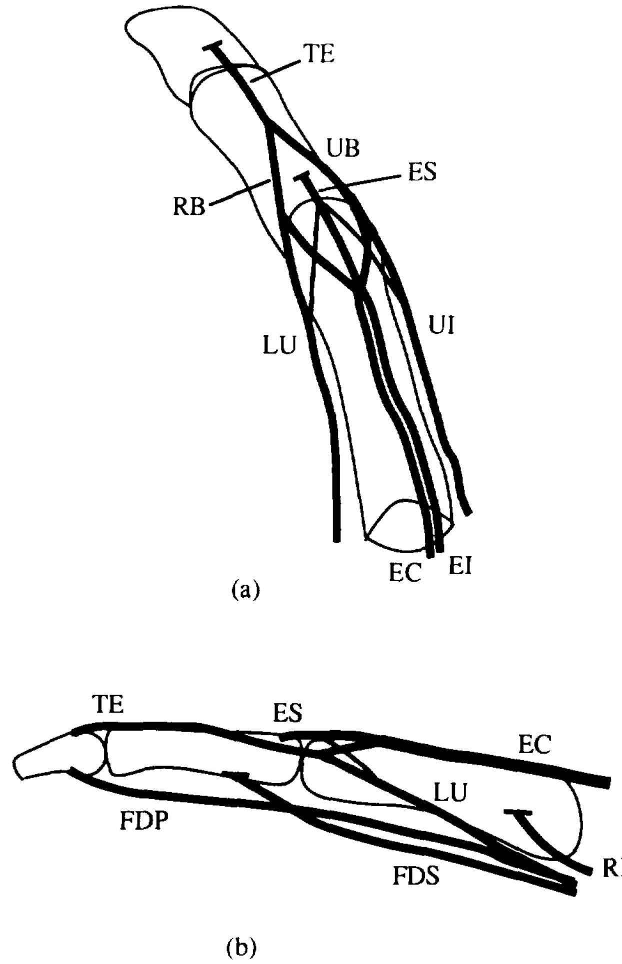

Figure 2 Tendons of the index finger. (a) The extensor mechanism. (b) A radial view

flexion. To solve the indeterminate problem, several simplifying assumptions were made. Equilibrium of the DIP joint was not considered. Subjects were asked to apply maximum force to a circular section transducer. While doing so, they were filmed from two orthogonal directions, to obtain the necessary skeletal geometrical information. In a later paper[4], a modified and extended analysis of the same and other tests predicted an average PIP joint reaction force of 4.6*P* and MP reaction force of 5.5*P* during pinch.

Weightman and Amis[5], introduced a 2D model for determining the variation of the joint forces with posture change. The same four constraint equations given by Chao and An[2] were used with an additional assumption that the long extensor tendons are relaxed. The tensions developed in the intrinsic muscles were assumed to be in proportion to the PCSA of the muscles and therefore, a general intrinsic tension (I) could be used, thus, making the model statically determinate with three unknown tensions FDP, FDS and I. Tendon moment arms and angles, were calculated, for each finger configuration, from the normative model of the human hand developed by An *et al.*[6]. Joint reaction forces, ranging from 6*P* to 3.5*P* for the MP and PIP joints, and from 3*P* to 2*P* for the DIP joint were determined. All forces decreased with finger flexion.

Lee and Rim[7], used linear programming to maximize the external forces that each of the phalanges of the middle finger can apply. The attempt was to predict maximum finger forces during cylindrical grasps. Tendon moment arms were taken to be dependent on flexion angles according to Landsmeer's models[8]. Passive muscle forces were included as lower bounds, and muscle force-length relationships were incorporated. Constraint equations derived from the anatomy were used. Good agreement with measured forces was obtained for postures with moderate PIP joint angles.

All of the above mentioned studies, relate to static postures of the fingers. A two dimensional dynamic model of interphalangeal coordination was suggested by Buchner *et al.*[9] The moments at the joints required to achieve a specified trajectory of free sagittal motion were equated to the moments supplied by the muscles. The moment arms were taken to be dependent on the flexion angles. Coefficients for the excursion models were approximated from data on the middle finger, yielding large excursions. The extensor mechanism was highly simplified to aid in the analyses. Constraint equations including a term representing the elasticity of extensor ligaments were introduced. Two optimization approaches were used, linear and non-linear, to minimize the sum of muscle stresses during free motion of phalangeal flexion. A hypothetical trajectory was used to examine the model.

In this study we introduce a 3 dimensional dynamic model for the index finger. Using a non-linear optimization approach the model predicts tendon forces needed to produce a specified motion and interaction with the environment. The finger is considered an isolated system (muscle dynamic characteristics are not included) with the goal of obtaining the "actuator" forces that produce the required dynamic behaviour. A minimal number of simplifications and assumptions are performed (the retinacular ligaments are not included and the wrist is assumed to remain at a constant position), and all the tendons and intrinsic muscles of the index finger considered (see *Table 1* and *Figure 2*). Coefficients of the models of tendon excursions are computed from experimental measurements performed by An *et al.*[10], thus yielding reliable excursions and moment arms. A new set of constraint equations is introduced including the variable contribution of the muscles to the extensor mechanism and the elasticity of the ligaments. The model is tested using data from a rapid pinch experiment[11] as well as a hypothetical trajectory of disc rotation. Results are qualitatively compared to EMG data from Long[12] and Long *et al.*[13].

TENDON DISPLACEMENT AND MOMENT ARM

An *et al.*[6], presented force potential and moment potential parameters, measured via X-ray films, to describe the contribution of each tendon in the force analysis. Radiography methods for measuring tendon positions can also be found in Berme *et al.*[3], though, for dynamic analysis, where moment arms vary with the joint angles, use of tendon excursion models is more convenient. The moment arms, can then be computed as the first order derivatives of the tendon displacement with respect to the joint angle[14,15]. Work by Brand *et al.*[14], Armstrong and Chaffin[16] and An *et al.*[10] suggests that Landsmeer's Model I[8] is well suited for describing extensor tendon excursions in the flexing finger. The equation used to represent displacement is

$$E = -r\phi \qquad (1)$$

where E denotes the displacement, r is the radius of the curved articular surface and ϕ is the joint angle. The minus sign is used since negative values represent tendons that elongate. The EC and EI at the MP joint, the ES at the PIP joint

Table 1 Tendons and intrinsic muscles of the index finger

Joint	Unknown tendon and intrinsic muscle forces
DIP	Terminal extensor (TE)
	Flexor digitorum profundus (FDP)
PIP	Extensor slip (ES)
	Radial band (RB)
	Ulnar band (UB)
	Flexor digitorum superficialis (FDS)
	Flexor digitorum profundus (FDP)
MP	Extensor digitorum Communis (EC)
	Extensor indicis (EI)
	Radial interosseous (RI)
	Ulnar interosseous (UI)
	Lumbrical (LU)
	Flexor digitorum superficialis (FDS)
	Flexor digitorum profundus (FDP)

and the TE at the DIP joint are included in this group. For the flexor group, which includes the FDP and the FDS Landsmeer's model III[8] is chosen[6,7]. Thus,

$$E = \phi d + 2y\left\{1 - \frac{\phi/2}{\tan(\phi/2)}\right\} \tag{2}$$

where d is a distance from the straight part of the tendon to the long axis, and y denotes a distance from the end of the straight part to the joint centre, measured along the axis of the bone[8]. Buchner *et al.*[9], approximated equation (2) by a second order polynomial. Hence,

$$E = (b + h\phi)\phi \tag{3}$$

where b and h are constants. For the current model, Equation (3) is used to represent only the displacement of the intrinsic muscles, during flexion-extension, as proposed by Lee and Rim[7]. Equation (3) is also chosen to represent displacement of all the tendons with respect to abduction-adduction motions. This choice seems reasonable in view of the data of An *et al.*[10] and the fact that equation (3) is a generalization of Equation (1). A subscript, a, will be used in the models dependent on abduction-adduction motion, with θ being the adduction angle. The coupling of the excursions due to adduction-abduction and flexion-extension motions is assumed negligible.

The problems relating to the displacement models, are how to determine the coefficients and how to calculate the total tendon excursion, from the individual excursions around each joint. Special attention must be paid to the rather complex extensor mechanism[17] (see *Figure 2*).

We relate first to the problem of determining total tendon excursions from the individual components and the relations between the excursions of the different tendons. For the flexor muscles, total excursion is simply the sum of their excursions around each joint.

$$\begin{aligned} E^{FDP} = {} & \phi_1 d_1^{FDP} + 2y_1^{FDP}\left\{1 - \frac{\phi_1/2}{\tan(\phi_1/2)}\right\} \\ & + \phi_2 d_2^{FDP} + 2y_2^{FDP}\left\{1 - \frac{\phi_2/2}{\tan(\phi_2/2)}\right\} \\ & + \phi_3 d_3^{FDP} + 2y_3^{FDP}\left\{1 - \frac{\phi_3/2}{\tan(\phi_3/2)}\right\} \\ & + (b_a^{FDP} + h_a^{FDP}\,\theta)\theta \end{aligned} \tag{4a}$$

$$\begin{aligned} E^{FDS} = {} & \phi_1 d_1^{FDS} + 2y_1^{FDS}\left\{1 - \frac{\phi_1/2}{\tan(\phi_1/2)}\right\} \\ & + \phi_2 d_2^{FDS} + 2y_2^{FDS}\left\{1 - \frac{\phi_2/2}{\tan(\phi_2/2)}\right\} \\ & + (b_a^{FDS} + h_a^{FDS}\theta)\theta \end{aligned} \tag{4b}$$

The extensor mechanism is more articulate than the flexors (*Figure 2*) and a more elaborate consideration is needed. Starting at the distal connections to the bones, it is clear that the excursion of the TE is a function of DIP rotation only, and that of the ES, a function of PIP rotation only.

$$E^{TE} = -\,r^{TE}\phi_3 \tag{4c}$$

$$E^{ES} = -\,r^{ES}\phi_2 \tag{4d}$$

Moving proximally from the terminal extensor, the lateral bands are next. Both Buchner *et al.*[9] and Lee and Rim[7], related to the lateral bands as being one (total symmetry is assumed). In the current model, the attempt is to be as detailed as possible, therefore, both the radial band and ulnar band are considered, and are taken to be distal to the LU and UI connections. The excursions of these bands are a function of PIP rotation with the addition of the excursion of the terminal extensor.

$$E^{RB} = -\,(b^{RB} + h^{RB}\phi_2)\phi_2 + \beta^{RB}E^{TE} \tag{4e}$$

$$E^{UB} = -\,(b^{UB} + h^{UB}\phi_2)\phi_2 + \beta^{UB}E^{TE} \tag{4f}$$

The parameters β^{RB} and β^{UB}, introduced here, represent the geometrical relation between these bands and the terminal extensor, and will be determined together with the model coefficients (equation 9).

Buchner *et al.*[9], considered also the two interosseus muscles as being one, and ignoring their connection to the lateral bands, their excursion was taken to be a specific function of both the PIP and MP joint rotations. Lee and Rim[7], related to the interosseus separately. The excursion of both was taken to be a function of PIP rotation, and to include the excursions of the lateral band and TE. These considerations of the interossei are in contradiction to anatomical data on the index finger[18] which shows that the first RI, ends at the radial side of the proximal phalanx, thus depending on MP rotation, whilst the UI normally connects to the dorsal digital expansion. Stack[17], even refers to the interossei as being proximal and distal rather than radial and ulnar or dorsal and palmar. These facts, are further emphasized in the data of An *et al.*[10], showing that for the RI, no excursions were measured during flexion of the PIP and DIP joints. Taking these conclusions into account for our model, the excursion of the RI is taken to be a function of MP rotation only, whilst the UI is considered the ulnar counterpart to the LU and therefore also a function of the UB excursion.

$$\begin{aligned} E^{RI} = {} & (b^{RI} + h^{RI}\phi_1)\phi_1 \\ & - (b_a^{RI} + h_a^{RI}\theta)\theta \end{aligned} \tag{4g}$$

$$\begin{aligned} E^{UI} = {} & (b^{UI} + h^{UI}\phi_1)\phi_1 \\ & + (b_a^{UI} + h_a^{UI}\theta)\theta + E^{UB} \end{aligned} \tag{4h}$$

$$\begin{aligned} E^{LU} = {} & (b^{LU} + h^{LU}\phi_1)\phi_1 \\ & - (b_a^{LU} + h_a^{LU}\theta)\theta \\ & + E^{RB} - E^{FDP} \end{aligned} \tag{4i}$$

The excursion of the FDP is deducted from the total excursion of the LU, since the origin of the LU is on the FDP.

The total displacements of the EC and EI are a function of MP rotation as well as whatever displacement is passed down from the extensor mechanism. If the excursion of the lateral bands is considered to be identical to that of the ES[7], then this contribution is added to the long extensor. If however, this ideal case is not assumed[9], then the maximal excursion (minimal negative excursion) is considered.

$$E^{EC} = -r^{EC}\phi_1 - (b_a^{EC} + h_a^{EC}\theta)\theta + \min[E^{ES}, E^{UB} + (1-\beta^{UB})E^{TE}, E^{RB} + (1-\beta^{RB})E^{TE}] \quad (4j)$$

$$E^{EI} = -r^{EI}\phi_1 + (b_a^{EI} + h_a^{EI}\theta)\theta + \min[E^{ES}, E^{UB} + (1-\beta^{UB})E^{TE}, E^{RB} + (1-\beta^{RB})E^{TE}] \quad (4k)$$

To complete the calculation of the excursions and of the tendon moment arms, the coefficients of the different functions must be determined. The coefficients given by Lee and Rim[7] are for the middle finger and not the index finger. Buchner *et al.*[9] used only equations (1) and (3) to describe the excursions, and obtained their coefficients by factorization of coefficients for the middle finger, without verifying the results with any data on the index finger. To improve on this, an attempt is made at calculating the coefficients and verifying results, using the data of An *et al.*[10]. This data was collected from cadaver fingers. Each joint was rotated to different flexion or adduction angles, and the excursion of each of the tendons was measured separately, while there was no load on the other tendons. The data presented in the paper is not the complete data collected, and includes only excursions of the seven extrinsic tendons and intrinsic muscles, for 100° rotations of each of the joints, and average moment arms for the range of motion. Since the above data is averaged, it can be used to obtain directly, with reliable results, only the coefficients of the models whose moment arms have a linear description (equations 1 and 3).

The following procedure is used; First, the excursion model of the muscle for flexion or adduction of 100° is compared to that given in the data.

$$E|_{\delta=100°} = E_D \quad (5)$$

This yields one equation with either one or two unknown coefficients depending on the model. The second equation, is derived from the data on average moment arm. The average is considered to be the integral of the moment arm over the range of motion divided by the angle of motion.

$$\overline{M}_D = \frac{1}{\delta_R}\int_0^{\delta_R} M(\delta_i)\, d\delta_i \quad (6)$$

Where $\overline{M}_D$ is the average moment arm given in the data. The moment arm around a certain joint, is the partial derivative of the elongation with respect to that joint's angle of rotation. Equation (6) thus yields,

$$\overline{M}_D = \frac{1}{\delta_R}\int_0^{\delta_R} \frac{\partial E(\delta_i)}{\partial \delta_i}\, d\delta_i = \frac{1}{\delta_R}[E(\delta_R) - E(0)] = \frac{1}{\delta_R}E(\delta_R) \quad (7)$$

which is an additional equation dependent on the model coefficients. For those muscles, modeled by equation (3), both coefficients can be found by solving equations (5) and (7). For those muscles modeled by equation (1), the average value obtained from equations (5) and (7) is taken.

To obtain the coefficients of the models described by equation (2), the data of Lee and Rim[7], for the middle finger, was factored to obtain the excursions measured by An *et al.*[10]. To further validate this approach the average moment arms with the new coefficients were computed and verified to be within a distance of one standard deviation from the averages reported.

As previously mentioned, An *et al.*[10], do not include data on the extensor slip, lateral bands, or terminal extensor. We derive this information, from the excursions of the EC, EI, UI and LU for flexion of the PIP and DIP joints, using the following procedure. (The EC and EI, which form the long extensor of the index finger, have almost identical excursions during flexion-extension. For the following analyses we relate, therefore, to the LE using the average of the data measured for the EC and EI.)

Data for DIP flexion ($\phi_1 = \phi_2 = 0$). For DIP flexion, the ES is considered to be slack. The excursion measured for the LE totally results therefore, from the excursion of the TE, thus yielding,

$$E^{TE} = E^{LE}|_{DIP} \quad (8)$$

During the measurements, only the muscle being measured, was loaded. Therefore, the excursion of the FDP is not considered here for calculating the excursion of the LU. Since also the other joints are not flexed, the β parameters can be determined from the measured excursions of the LU and UI (see equations 4e–i).

$$\beta^{RB} = \left.\frac{E^{LU}}{E^{TE}}\right|_{DIP} \quad (9a)$$

$$\beta^{UB} = \left.\frac{E^{UI}}{E^{TE}}\right|_{DIP} \quad (9b)$$

Data for PIP flexion ($\phi_1 = \phi_3 = 0$). We assume, that for PIP flexion only, all the excursion of the LE, results from the excursion of the ES. We can therefore write,

$$E^{ES} = E^{LE}|_{PIP} \quad (10)$$

In addition, we assume, that all the excursion measured for the LU and UI, results from that of the RB and UB respectively. Thus yielding,

$$E^{RB} = E^{LU}|_{PIP} \quad (11a)$$

$$E^{UB} = E^{UI}|_{PIP} \quad (11b)$$

Values of all the coefficients obtained with the methods described are given in *Table 2*.

FORCE CONSTRAINT EQUATIONS

To assist in solving the indeterminate set of static/dynamic equilibrium equations a set of constraint equations is derived. These equations

Table 2 Coefficients of excursion models (mm)

Joint	Tendon	r	b	h	d	y	b_a	h_a
DIP	TE	1.88	–	–	–	–	–	–
	FDP	–	–	–	2.97	3.96	–	–
PIP	ES	2.92	–	–	–	–	–	–
	RB	–	2.54	−0.47	–	–	–	–
	UB	–	1.7	0.57	–	–	–	–
	FDS	–	–	–	4.13	6.73	–	–
	FDP	–	–	–	5.76	7.5	–	–
MP	EC	8.3	–	–	–	–	2.08	−0.09
	EI	8.82	–	–	–	–	0.59	0.8
	RI	–	5.62	−1.29	–	–	5.63	0.54
	UI	–	18.76	−8.16	–	–	5.77	0.03
	LU	–	12.53	−2.17	–	–	4.96	−0.18
	FDS	–	–	–	9.56	8.14	1.1	0.68
	FDP	–	–	–	8.32	8.32	0.52	0.66

define the relationships between the forces of the extensor mechanism, where the tendons interconnect. A combination of previous methods is used. Chao and An[2], suggested the following equations based on a study of the anatomical structure.

$$F^{TE} = F^{RB} + F^{UB} \tag{12a}$$

$$F^{RB} = \frac{2}{3}F^{LU} + \frac{1}{6}F^{LE} \tag{12b}$$

$$F^{UB} = \frac{1}{3}F^{UI} + \frac{1}{6}F^{LE} \tag{12c}$$

$$F^{ES} = \frac{1}{3}F^{LU} + \frac{1}{6}F^{LE} + \frac{1}{3}F^{RI} + \frac{1}{3}F^{UI} \tag{12d}$$

Weightman and Amis[5] used the same set of constraints, eliminating only the force of the LE, under the assumption that during pinch this tendon is slack. Lee and Rim[7] used a similar set of constraints for the middle finger. Besides the force coefficients being different, an additional contribution of the RI to the force of the RB is considered, and since total symmetry is assumed, the RB and UB are assumed to bear equal forces. Buchner *et al.*[9], suggested a different set of constraints including the following equation:

$$(2\alpha - 1)F^{LE} + F^{ES} - F^{TE} = 2K\varepsilon \tag{13a}$$

with,

$$\varepsilon = E^{LB} + E^{TE} - E^{ES} \tag{13b}$$

An interesting concept introduced in this equation is the parameter α, representing the fraction of force transmitted by the LE to each of the lateral bands. This parameter, is considered in the paper to be a variable, changing perhaps due to geometrical changes during movement, and is estimated together with the muscle forces using a non-linear optimization algorithm. An additional concept introduced, is that of elasticity (K) originating from the ligaments connecting the different parts of the extension mechanism, and causing an additional force due to the relative motion (ε) between the lateral bands and the ES. In these equations, however, the interossei are assumed not to connect to the extensor mechanism.

In the present model, as cited above, a combination of the two approaches is used. The constraint equations are based on equation (12), though it is assumed that the coefficients may change due to geometrical changes during motion. The force of the RI is not included in the equations for the same reasons mentioned in the previous section. Elasticity of the extensor mechanism is included. It is assumed that an equal fraction of the extensor's force is conveyed to each of the lateral bands. The constraint equations are thus given by,

$$F^{TE} = \chi^{RB}F^{RB} + \chi^{UB}F^{UB} \tag{14a}$$

$$F^{RB} = \alpha^{LU}F^{LU} + \alpha^{LE}F^{LE} - K\varepsilon^{RB} \tag{14b}$$

$$F^{UB} = \alpha^{UI}F^{UI} + \alpha^{LE}(F^{EC} + F^{EI}) - K\varepsilon^{UB} \tag{14c}$$

$$F^{ES} = (1 - \alpha^{LU})F^{LU} + (1 - 2\alpha^{LE})(F^{EC} + F^{EI}) + (1 - \alpha^{UI})F^{UI} + K(\varepsilon^{RB} + \varepsilon^{UB}) \tag{14d}$$

where χ^{RB} and χ^{UB} are cosine terms accounting for the convergence angles of the RB and UB on to the TE. The convergence angles were estimated from anatomical descriptions of the musculature[18] and were found to be ~ 10°, thus, yielding cosine terms of ~ 0.985. This result is in accordance with data from An *et al.*[6] showing that the force potential parameters of the RB and UB, in the direction of the major finger axis, are 0.992 and 0.995 respectively. ε^{RB} and ε^{UB} are the relative displacements between the ES and the RB and UB respectively. The α coefficients are estimated together with the forces using a non-linear optimization algorithm. The value of the elasticity K is taken from Buchner *et al.*[9].

SIMULATION

The dynamic equations of an open chain of rigid links can be derived using either the Lagrange or Newton–Euler methods. For the simulation, a recursive Newton–Euler method is used[19], yielding the joint driving moments (τ) required to produce the given motion. These driving moments are created by the forces in the muscles crossing each of the joints, multiplied by their respective moment arms.

$$\tau = WF_m \tag{15}$$

The elements of the moment arm matrix W can be evaluated, by differentiating the excursion of each of the tendons with respect to each joint, as shown previously. The vector of muscle forces F_m is left to be calculated by solving equation (15). It is clear though, that equation (15) is indeterminate since τ is a vector in the dimension of the degrees of freedom n (for the finger $n = 4$), and F_m is in the dimension of the number of unknown tendon forces ($u = 11$). The additional constraint equations (14a–d) are also considered yielding eight equations with 14 unknowns. To solve this problem, a non-linear optimization technique is used. Many minimization criteria have been proposed[2,20] with muscle stress clearly the most popular[20]. Buchner *et al.*[9] proposed using the muscle stresses squared which accentuates the differences between the tendons. To enable comparison with their results, this criterion has been chosen.

Muscle stress is defined as the muscle force divided by its physiological cross sectional area (PCSA). The cost function is, therefore, defined by,

$$J_c = \sum_{i=1}^{u} \left(\frac{F_{m_i}}{PCSA_i} \right)^2 \qquad (17)$$

The data for the PCSA of the muscles in the index finger was taken from Chao and An[2]. Upper limits on the muscle stresses can also be incorporated into the simulation as in Chao and An[2] or Lee and Rim[7]. To examine the credibility of the model, two simulations were performed, one of pinch action and the other of disc rotation.

Pinch

The pinch action of a human index finger is simulated, based on data from Cole and Abbs[11]. In their study, subjects were asked to perform pinch actions with the index finger and thumb. The rotation angles of the PIP and MP joints were measured as well as the pinch force. The DIP joint was fixed at a constant 20° flexion angle. Subjects were asked to attempt to produce a pinch force of about 1N in repetitive trials. In the initial position, all joints were flexed ~ 20° with the finger and thumb pulps separated by ~ 4–7 cm. Data for the current simulation were estimated from representative signals presented in the paper. The angular flexion trajectories of the three joints of the index finger; as well as the pinch force, are depicted in *Figure 3*. The pinch force is assumed to remain vertical throughout the action.

The goal of our simulation is to determine the index finger muscle forces used to produce the given trajectory and pinch force. Only the index finger is simulated. It is considered an open chain of rigid links pressing against a spring-dashpot system (*Figure 1*), which represents fingertip compliance. The contact force is assumed to be vertical at all times, and the palm is assumed to be elevated 50°. In the absence of additional data the finger is assumed to be completely abducted during the motion. The dynamic parameters of the finger, such as segment length, mass and inertia, were taken from Buchner *et al.*[9].

Disc rotation

To observe the action of the muscles during abduction–adduction motions, a simulation of disc rotation is performed. Since no experimental data of trajectories and forces, during such an action, could be found in the literature, hypothetical trajectories and forces were used. The finger is assumed to rotate 45° with a circular disc and roll on it while doing so. Thus, the external forces on the finger, rotate with respect to it (*Figure 4*). The MP joint is assumed to flex slightly and the PIP and DIP extend slightly during the motion. The palm is assumed to be elevated 70°.

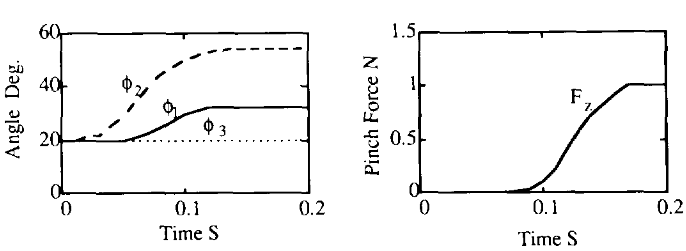

Figure 3 Signals from pinch experiment. Angular position of the joints and vertical pinch force

RESULTS AND DISCUSSION

Pinch

Tendon excursions for the simulated motion, are depicted in *Figure 5*. These are, of course within the range of excursions reported by An *et al.*[10]. The initial excursions are for the initial posture of 20° flexion of all joints. The final, maximal, excursions are about half the magnitude of those obtained, for the same position, using the coefficients presented by Buchner *et al.*[9], and seem highly more reasonable. Note that the difference between the excursions of the FDP and FDS remains more or less constant because the DIP is fixed at a constant angle and therefore does not contribute to FDP excursion.

The tendon forces computed by the optimization algorithm are presented in *Figure 6*. The three phases; free motion, motion with external force and external pinch force without motion,

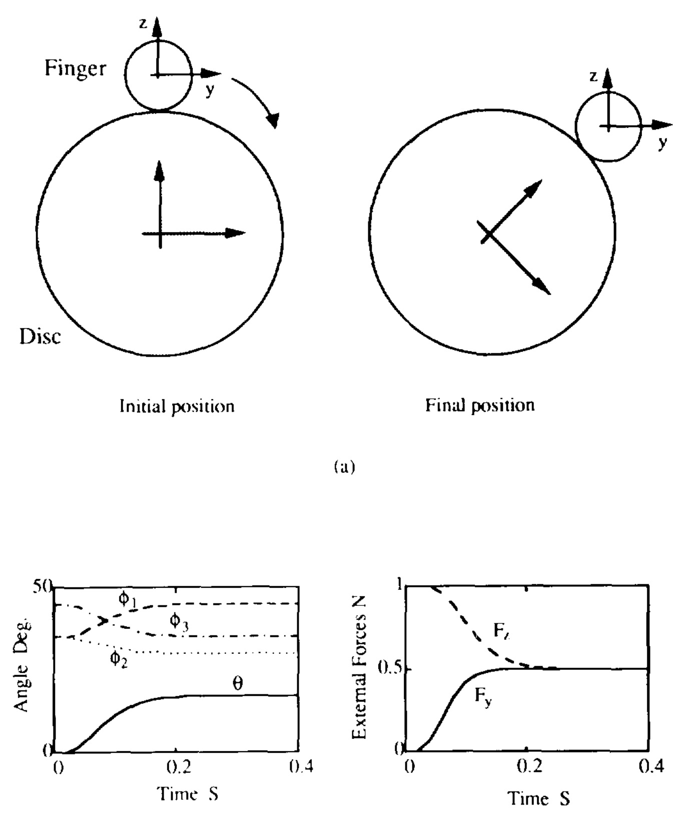

Figure 4 Disc rotation. (a) Schematic planar representation. (b) Angular position and external force

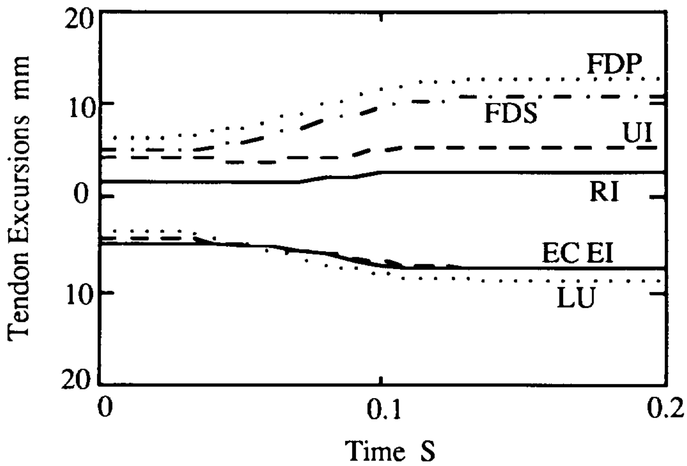

Figure 5 Tendon excursions during simulated pinch motion

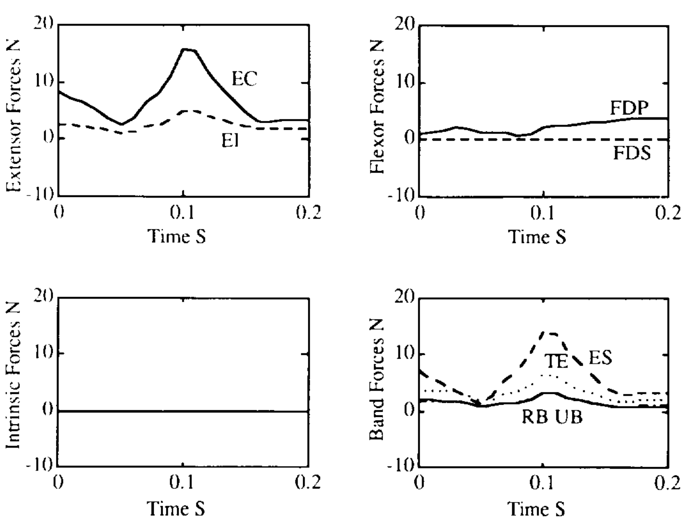

Figure 6 Tendon forces during simulated pinch motion

should be distinguished (see *Figure 3*). Note that during the deceleration in free flexion motion, the forces of the extensors increase considerably. This is in accordance with EMG data and the idea suggested by Long[12], that the extensor digitorum contributes a braking influence during flexion. Once the external force takes effect the extensor forces reduce. The constraint of no adduction motion can account for the difference between the forces of the two extensors.

The FDS is seen to be silent during the pinch action. For free motion this is in accordance with EMG data presented by Long[12]. For the pinch action itself, both Long *et al.*[13] and Williams *et al.*[18] state that the FDS assists only in more powerful and rapid gripping. The pinch force of 1 N in this simulation is small compared to the possible maximum pinch forces of 30 to 100 N reported in several papers (see Weightman and Amis[5], for a review), thus explaining the results. Participation of the FDS for larger forces is examined later.

The three intrinsic muscles also remain silent during all phases of the motion. This too, is in accordance with EMG experimental data[12,13], showing that the intrinsics do not participate actively during free flexion motion and participate partially during strong pinch.

The bands of the extensor mechanism participate in a similar manner to the long extensor, in moderating the flexion action. The ES bears particularly large forces originating mainly from the elasticity of the extensor mechanism itself (equation 14d). This large force (8N) is needed due to the relatively small moment arm of the ES (*Table 2*). The TE is also active, supporting the distal phalanx. The forces of the RB and UB are identical maintaining symmetry of the extensor mechanism.

The behavior of the α coefficients (equation 14) is shown in *Figure 7*. Note that the LU coefficient remains approximately at its initial value of 0.67 throughout the motion. The UI coefficient remains at its initial value of 0.333 during the free motion but decreases with the initiation of pinch. This decrease, however, causes minor changes to the muscle forces since the force of the UI is practically zero. The coefficient of the LE does not originate from the assumed initial value of 0.33 but from a lower value of 0.15 thus transmitting more force than expected to the ES. This value remains more or less constant during the motion and the initiation of pinch.

The joint forces at the MP and PIP joints are almost equivalent during all phases of the motion and larger than that at the DIP joint (*Figure 8*). This behaviour is similar to that reported by Weightman and Amis[5] for static pinch. The magnitude of the forces (6–9 N at the static pinch phase) are also within the range of forces reported in previous studies (2–9 N).

To examine the participation of the FDS and intrinsic muscles in stronger pinch actions an additional simulation was performed. In this simulation the magnitude of the pinch force was increased by a factor of 6. The optimized muscle driving forces are shown in *Figure 9*. Note that the change of pinch force only, is somewhat artificial since for increased pinch force it is likely to expect certain changes in the trajectory as well. The participation of the FDS and intrinsic muscles is evident (for a slightly smaller force, only the

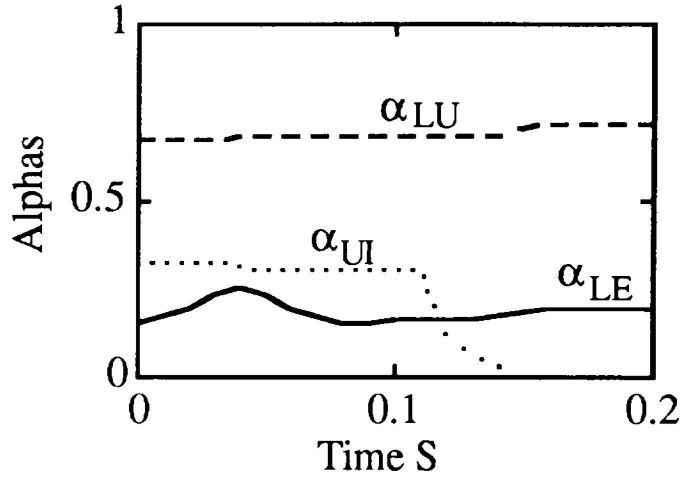

Figure 7 Variation of α coefficients

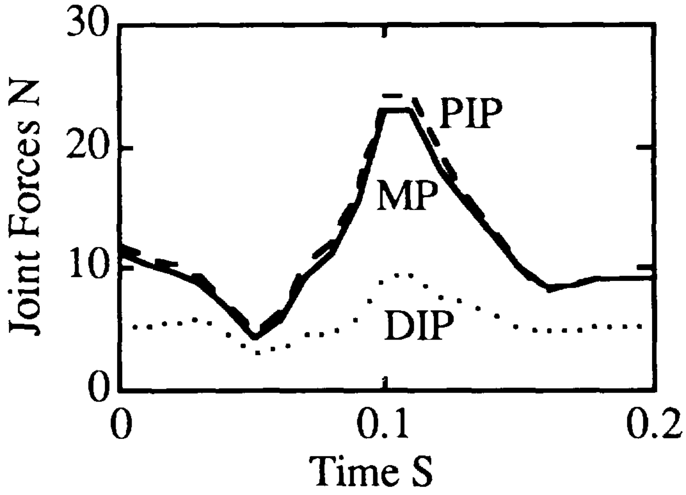

Figure 8 Variation of joint forces

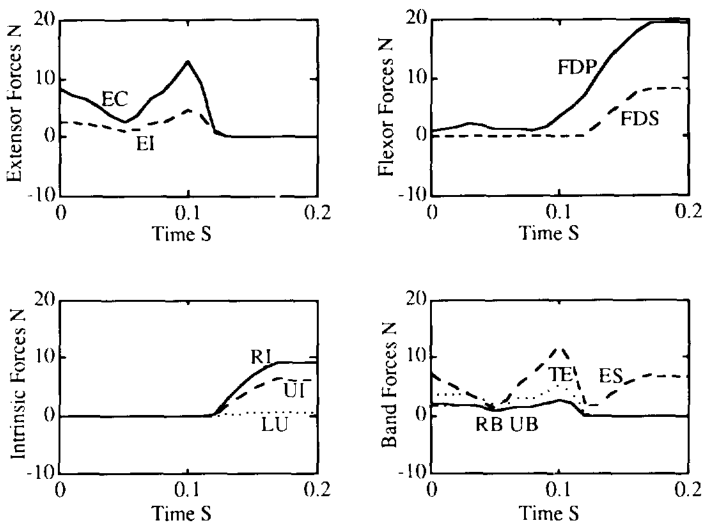

Figure 9 Tendon forces during simulated pinch motion for vertical pinch force increased by factor of six

additional force of the FDS was obtained). Note the relative contributions of the RI, UI and LU, which are in full accordance with EMG data of Long *et al.*[13].

Disc rotation

The tendon forces during disc rotation, are presented in *Figure 10.* The EC, which is not an adductor, is shown to produce rather large forces which are probably needed for the extension of the PIP and DIP joints (see also forces in the bands). The FDP is the main producer of the grip force, and may contribute somewhat to the adduction motion. The main adduction motion is most likely produced by the UI which would otherwise be silent. The EMG data of Long *et al.*[13] concentrates on the intrinsic muscles, indeed showing that the UI is the most active during clockwise disc rotation with the right hand.

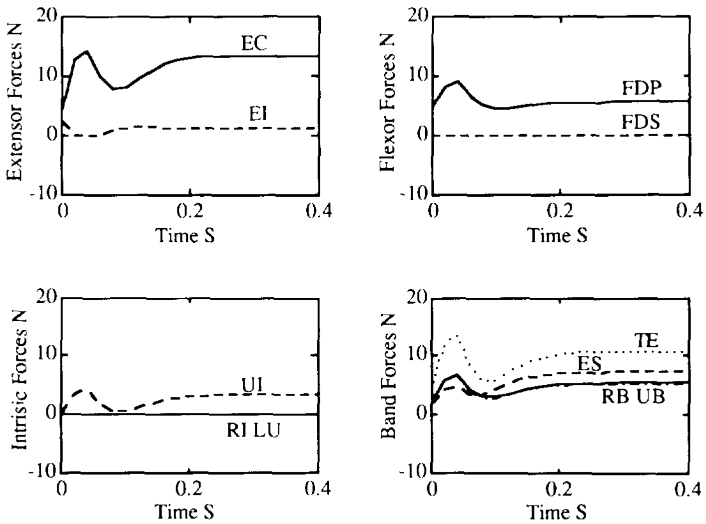

Figure 10 Tendon forces during simulated disc rotation

SUMMARY AND CONCLUSIONS

An extended dynamic model of the biomechanics of the index finger for flexion–extension and abduction–adduction motion has been introduced. The model takes into account all the tendons in the finger and relates to their varying moment arms during motion. A new set of moment arm coefficients and elongation equations was derived based on experimental results in previous studies. Constraint equations using variable coefficients were introduced and an optimization approach used to obtain the tendon forces required for any given motion and external force. The model and optimization approach were tested with data from a rapid pinch experiment, and good correlation was obtained with respect to EMG data in the literature. It is our conclusion therefore, that this model produces with reasonable likelihood the tendon forces developed in the index finger.

ACKNOWLEDGMENT

This research was supported by The Fund for the Promotion of Research at the Technion, The Segal Foundation, and the Walter and Sandra Kaye Foundation.

REFERENCES

1. Chao EY, Opgrande JD and Axmear FE. Three-dimensional force analysis of finger joints in selected isometric hand functions. *J Biomechanics*, 1976, **9**, 387–396.
2. Chao EY and An KN. Graphical interpretation of the solution to the redundant problem in biomechanics. *Trans. ASME J Biomechanical Eng.*, 1978, **100**, 159–167.
3. Berme PW, Paul JP and Purves WK. A biomechanical analysis of the metacarpophalangeal joint. *J Biomechanics*, 1977, **10**, 409–412.
4. Purves WK and Berme N. Resultant finger joint loads in selected activities. *J Biomedical Eng.*, 1980, **2**, 285–289.
5. Weightman B and Amis AA. Finger joint force predictions related to design of joint replacements. *J Biomedical Eng.*, 1982, **4**, 197–205.
6. An KN, Chao EY, Cooney WP and Linscheid KL. Norma-

tive model of human hand for biomechanical analysis. *J Biomechanics*, 1979, **12**, 775–788.
7. Lee JW and Rim K. Maximum finger force prediction using a planar simulation of the middle finger. *Proc. Institute Mechanical Engineers Part H: J Engineering in Medicine*, 1990, **204**, 169–178.
8. Landsmeer JMF. Study in the anatomy of articulation 1. The equilibrium of the 'intercalated' bone, *Acta morph neerl.-scand.*, 1961, **3**, 287–303.
9. Buchner HJ, Hines MJ and Hemami H. A dynamic model for interphalangeal coordination. *J Biomechanics*, 1988, **21**, 459–468.
10. An KN, Veba Y, Chao EY, Cooney WP and Linscheid KL. Tendon excursion and moment arm of index finger muscles. *J. Biomechanics* 1983, **16**, 419–425.
11. Cole KJ and Abbs JH. Coordination of three-joint digit movements for rapid finger-thumb grasp. *J Neurophysiology*, 1986, **55**, 1407–1423.
12. Long C. Intrinsic-extrinsic muscle control of the fingers, *J Bone and Joine Surgery*, 1968, **50A**, 973–984.
13. Long C, Conrad PW, Hall EA and Furler SL. Intrinsic-extrinsic muscle control of the hand in power grip and precision handling. *J Bone and Joint Surgery*, 1970, **52A**, 853–867.
14. Brand PW, Cranor KC and Ellis JC. Tendon and pulleys at the metacarpo-phalangeal joint of a finger, *J Bone and Joint Surgery*, 1975, **57A**, 779–784.
15. Storace A and Wolf B. Functional analysis of the role of the finger tendons. *J Biomechanics*, 1979, **12**, 575–578.
16. Armstrong TJ and Chaffin DB. An investigation of the relationship between displacement of the finger and wrist joints, and the extrinsic finger flexor tendons, *J Biomechanics*, 1978, **11**, 119–128.
17. Stack HG. Muscle function in the fingers. *J Bone and Joint Surgery*, 1962, **44B**, 899–909.
18. Williams PL, Warwick R, Dyson M and Bannister LH. *Gray's Anatomy*, 37th ed., Longman Group, UK Limited, 1989.
19. Luh JYS, Walker MW and Paul RP. On line computational scheme for mechanical manipulators. *Trans. ASME J Dynamic Systems Measurement and Control*, 1980, **102**, 69–76.
20. Zajac F and Winters JM. Modeling musculoskeletal movement systems: Joint and body-segment dynamics, musculotendinous actuation, and neuromuscular control, *Multiple Muscle Systems–Biomechanics and Movement Organization*, JM Winters and Savio L-Y Woo editors, Springer-Verlag, New York, 1990.